

Distribution and seasonal evolution of supraglacial lakes on Shackleton Ice Shelf, East Antarctica: Supplementary Information

Jenifer F. Arthur, Chris R. Stokes, Stewart S.R. Jamieson, J. Rachel Carr, Amber A. Leeson

5

Table 1: Details of satellite imagery used in this study, including NDWI thresholds. Scenes used in subset area analysis are marked with a *.

Scene ID	Subset analysis	UTM Zone	Date	Satellite/sensor	Cloud cover (%)	Data cover (%)	NDWI Threshold
S2B_MSIL1C_20200101T021549_N0208_R117_T47DNG	*	47S	01/01/2020	Sentinel 2 MSI	54.4	45.6	0.25
S2B_MSIL1C_20200111T021549_N0208_R117_T47DNG	*	47S	11/01/2020	Sentinel 2 MSI	36	64	0.25
LC08_L1GT_110107_20200113_20200127		47S	13/01/2020	Landsat 8 OLI	0.02	99.8	0.25
LC08_L1GT_113106_20200118_20200128		47S	18/01/2020	Landsat 8 OLI	26.1	73.9	0.25
LC08_L1GT_112107_20200127_20200210		47S	27/01/2020	Landsat 8 OLI	2.8	97.2	0.25
S2B_MSIL1C_20200131T021549_N0208_R117_T47DNG	*	47S	31/01/2020	Sentinel 2 MSI	16.3	83.7	0.25
LC08_L1GT_112107_20200228_20200228	*	47S	28/02/2020	Landsat 8 OLI	0.06	99.9	0.25
LC08_L1GT_111106_20191101_20191114	*	47S	11/01/2019	Landsat 8 OLI	20.2	79.8	No lakes present
LC08_L1GT_111107_20191203_20191216	*	47S	03/12/2019	Landsat 8 OLI	0	100	No lakes present
LC08_L1GT_111107_20191219_20191226	*	47S	19/12/2019	Landsat 8 OLI	17.4%	82.6%	0.25
S2B_MSIL1C_20190105T024559_N0207_R103_T47DMG		47S	05/01/2019	Sentinel 2 MSI	27.6%	72.4%	0.25
S2B_MSIL1C_20190129T022559_N0207_R017_T47DPG		47S	29/01/2019	Sentinel 2 MSI	20%	80%	0.25
S2B_MSIL1C_20190129T022559_N0207_R017_T47DNG	*	47S	29/01/2019	Sentinel 2 MSI	20%	80%	0.25
LC08_L1GT_111107_20190218_20190218	*	47S	18/02/2019	Landsat 8 OLI	0%	100%	0.25
S2B_MSIL1C_20190228T022549_N0207_R017_T47DNG	*	47S	28/02/2019	Sentinel 2 MSI	16.8%	83.2%	0.25
S2A_MSIL1C_T47DNG_A013456_20180119T022550	*	47S	19/01/2018	Sentinel 2 MSI	10.9%	89.1%	0.25
S2A_MSIL1C_20180126T021551_N0206_R117_T47DNG	*	47S	26/01/2018	Sentinel 2 MSI	0.2%	99.8%	0.25
LC08_L1GT_113106_20180128_20180207		47S	28/01/2018	Landsat 8 OLI	1.9%	98.1%	0.21

S2A_L1C_T47DNG_A013742_20180208T022548	*	47S	08/02/2018	Sentinel 2 MSI	6.4%	93.6%	0.15
LC08_L1GT_111107_20180215_20180215	*	47S	15/02/2018	Landsat 8 OLI	0.07%	99.9%	0.20
LC08_L1GT_111106_20170127_20170214	*	47S	27/01/2017	Landsat 8 OLI	0.3%	99.7%	0.25
S2A_MSIL1C_20170130T024551_N0204_R103_T47DMG		47S	30/01/2017	Sentinel 2 MSI	15.5%	84.5%	0.25
S2A_MSIL1C_T47DNG_A008408_20170131T021548	*	47S	31/01/2017	Sentinel 2 MSI	1.7%	98.3%	0.25
S2A_MSIL1C_20170131T021551_N0204_R117_T47DPG		47S	31/01/2017	Sentinel 2 MSI	6.7	93.3	0.25
S2A_MSIL1C_T47DPG_A008408_20170131T021548		47S	31/01/2017	Sentinel 2 MSI	6.6%	93.4%	0.25
LC08_L1GT_111107_20171229_20171229	*	47S	29/12/2017	Landsat 8 OLI	0%	100%	0.25
LC08_L1GT_111107_20170228_20170228		47S	28/02/2017	Landsat 8 OLI	9.5	95.5	0.25
LC08_L1GT_111107_20160109_20170405	*	47S	09/01/2016	Landsat 8 OLI	0.97%	99.03%	0.25
LC08_L1GT_111107_20160125_20170330	*	47S	25/01/2016	Landsat 8 OLI	0.3%	99.7%	0.25
LC08_L1GT_111106_20160226_20170329	*	47S	26/02/2016	Landsat 8 OLI	1.5%	98.5%	0.10
LC08_L1GT_111107_20150106_20180204_01_T2	*	47S	06/01/2015	Landsat 8 OLI	5.7%	94.3%	0.25
LC08_L1GT_111107_20150207_20180204	*	47S	07/02/2015	Landsat 8 OLI	17.9%	82.1%	0.25
LC08_L1GT_111107_20150223_20180204	*	47S	23/02/2015	Landsat 8 OLI	13.1%	86.9%	0.25
LC08_L1GT_111107_20140103_20170427	*	47S	03/01/2014	Landsat 8 OLI	27.2%	72.8%	0.25
LC08_L1GT_111107_20140119_20170426	*	47S	19/01/2014	Landsat 8 OLI	14.3%	85.7%	0.25
LE07_L1GT_112106_20130115_20161126		47S	15/01/2013	Landsat 7 ETM+	24%	76%	0.25
LC08_L1GT_111107_20131202_20170428	*	47S	02/12/2013	Landsat 8 OLI	2.9%	97.1%	0.25
LE07_L1GT_111106_20120122_20161203		47S	22/01/2012	Landsat 7 ETM+	15%	85%	0.25
LE07_L1GT_111106_20120223_20161203	*	47S	23/02/2012	Landsat 7 ETM+	1%	99%	0.25
LE07_L1GT_111107_20120223_20161203	*	47S	23/02/2012	Landsat 7 ETM+	0%	100%	0.25
LE07_L1GT_111106_20110103_20161210		47S	03/01/2011	Landsat 7 ETM+	0%	100%	0.25
LE07_L1GT_111107_20110204_20161211	*	47S	04/02/2011	Landsat 7 ETM+	0%	100%	0.25
LE07_L1GT_112107_20110227_20161210		47S	27/02/2011	Landsat 7 ETM+	2%	98%	0.15
LE07_L1GT_111107_20111103_20161205	*	47S	03/11/2011	Landsat 7 ETM+	0	100	No lakes present

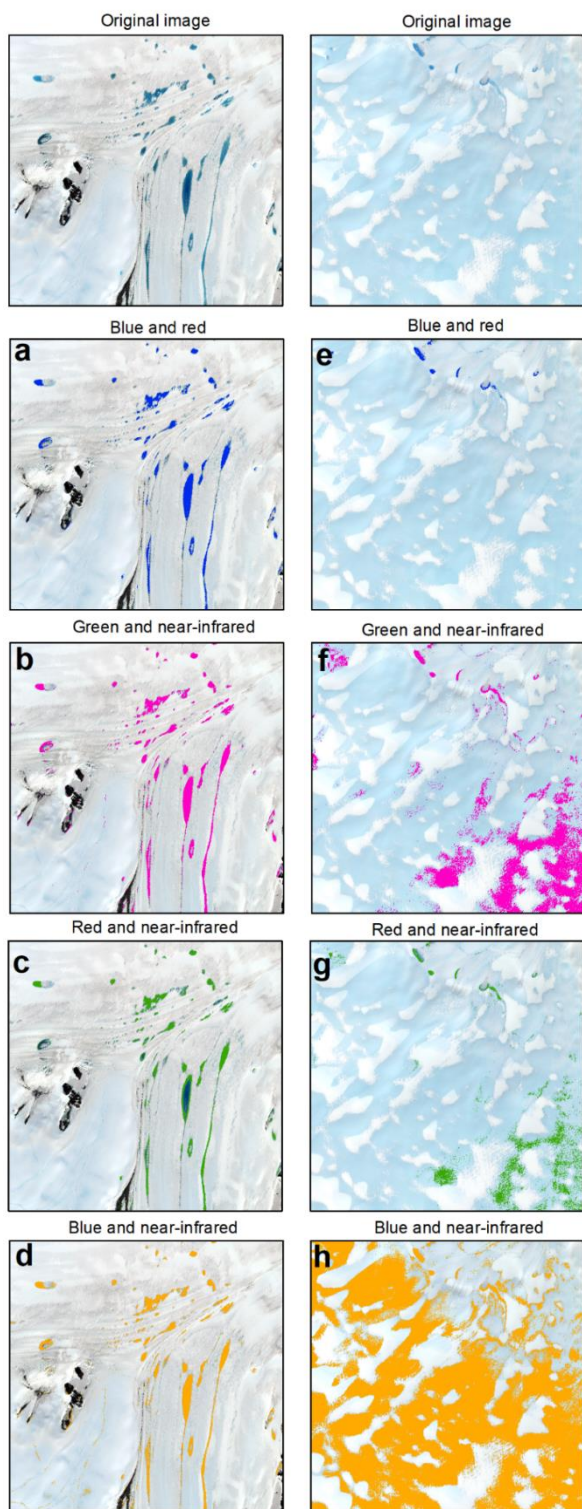
LE07_L1GT_111107_20111119_20161205	*	47S	19/11/2011	Landsat 7 ETM+	0	100	No lakes present
LE07_L1GT_111107_20111205_20161204	*	47S	5/12/2011	Landsat 7 ETM+	0	100	No lakes present
LE07_L1GT_110107_20100210_20161217		47S	10/02/2010	Landsat 7 ETM+	0%	100%	0.25
LE07_L1GT_113106_20100215_20161216	*	47S	15/02/2010	Landsat 7 ETM+	2%	98%	0.25
LE07_L1GT_113107_20100215_20161216	*	47S	15/02/2010	Landsat 7 ETM+	1%	99%	0.15
LE07_L1GT_111107_20100217_20161215	*	47S	17/02/2010	Landsat 7 ETM+	0%	100%	0.25
LE07_L1GT_112106_20100224_20161217	*	47S	24/02/2010	Landsat 7 ETM+	0%	100%	0.20
LE07_L1GT_112106_20101107_20161212	*	47S	07/11/2010	Landsat 7 ETM+	0%	100%	0.25
LE07_L1GT_114107_20090102_20161223		47S	02/01/2009	Landsat 7 ETM+	1%	99%	0.25
LE07_L1GT_111106_20091231_20161216		47S	31/12/2009	Landsat 7 ETM+	13%	87%	0.20
LE07_L1GT_113107_20080109_20161231		47S	09/01/2008	Landsat 7 ETM+	10%	90%	0.25
LE07_L1GT_111107_20080127_20161230		47S	27/01/2008	Landsat 7 ETM+	0%	100%	0.25
LE07_L1GT_111106_20080127_20161230		47S	27/01/2008	Landsat 7 ETM+	0%	100%	0.25
LE07_L1GT_111107_20081126_20161223	*	47S	26/11/2008	Landsat 7 ETM+	1	99	No lakes present
LE07_L1GT_111107_20081212_20161223	*	47S	12/12/2008	Landsat 7 ETM+	0	100	No lakes present
LE07_L1GT_112107_20070115_20170105		47S	15/01/2007	Landsat 7 ETM+	0%	100%	0.25
LE07_L1GT_113107_20070122_20170105	*	47S	22/01/2007	Landsat 7 ETM+	0%	100%	0.25
LE07_L1GT_113107_20070223_20170105		47S	23/02/2007	Landsat 7 ETM+	21%	79%	0.25
LE07_L1GT_112106_20061230_20170106		47S	30/12/2006	Landsat 7 ETM+	2%	98%	0.27
LE07_L1GT_112106_20040208_20170123		47S	08/02/2004	Landsat 7 ETM+	19%	81%	0.25
LE07_L1GT_112107_20040208_20170123		47S	08/02/2004	Landsat 7 ETM+	0%	100%	0.25
LE07_L1GT_112106_20021219_20170127		47S	19/12/2002	Landsat 7 ETM+	0%	100%	0.20
LE07_L1GT_112107_20021219_20170127		47S	19/12/2002	Landsat 7 ETM+	2%	98%	0.25
LE07_L1GT_111106_20000206_20170213	*	47S	06/02/2000	Landsat 7 ETM+	8%	92%	0.25
LE07_L1GT_111107_20000206_20170213	*	47S	06/02/2000	Landsat 7 ETM+	0%	100%	0.25
LT05_L1GS_114107_19910210_20170127		47S	10/02/1991	Landsat 5 TM	0%	100%	0.25

LT05_L1GS_114106_19910210_20170127		47S	10/02/1991	Landsat 5 TM	0%	100%	0.25
LT05_L1GS_112107_19910212_20170127		47S	12/02/1991	Landsat 5 TM	1%	99%	0.25
LT05_L1GS_112107_19910228_20170127		47S	28/02/1991	Landsat 5 TM	11%	89%	0.25
LT04_L1GS_112106_19891113_20170201		47S	13/11/1989	Landsat 4 TM	15%	85%	0.25
LT04_L1GS_112107_19891113_20170201		47S	13/11/1989	Landsat 4 TM	0%	100%	0.25
LM01_L1GS_119107_19740223_20180426		47S	23/02/1974	Landsat 1 MSS	6%	94%	0.15

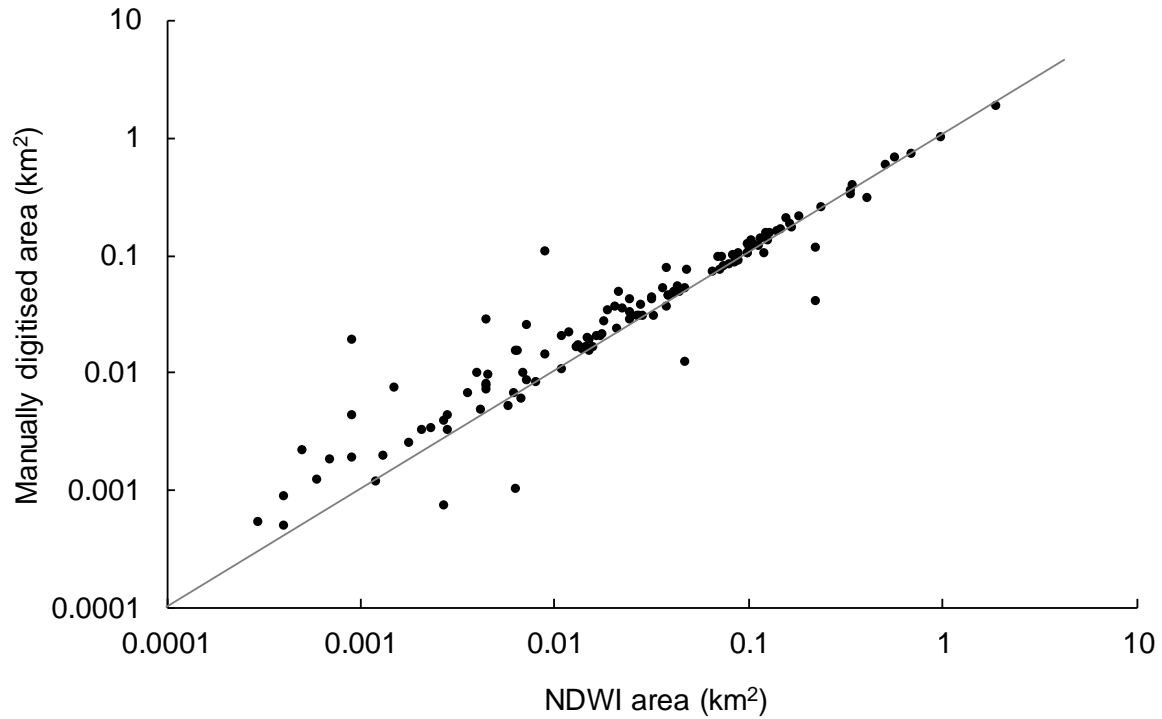
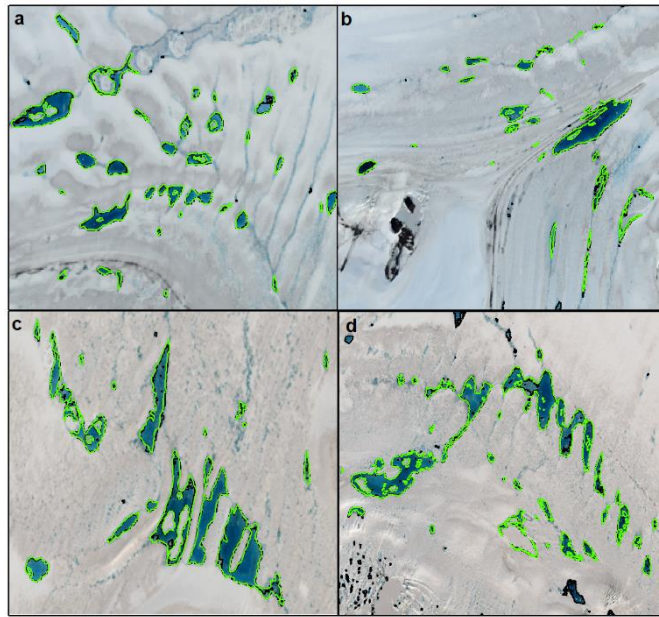
10

15

20



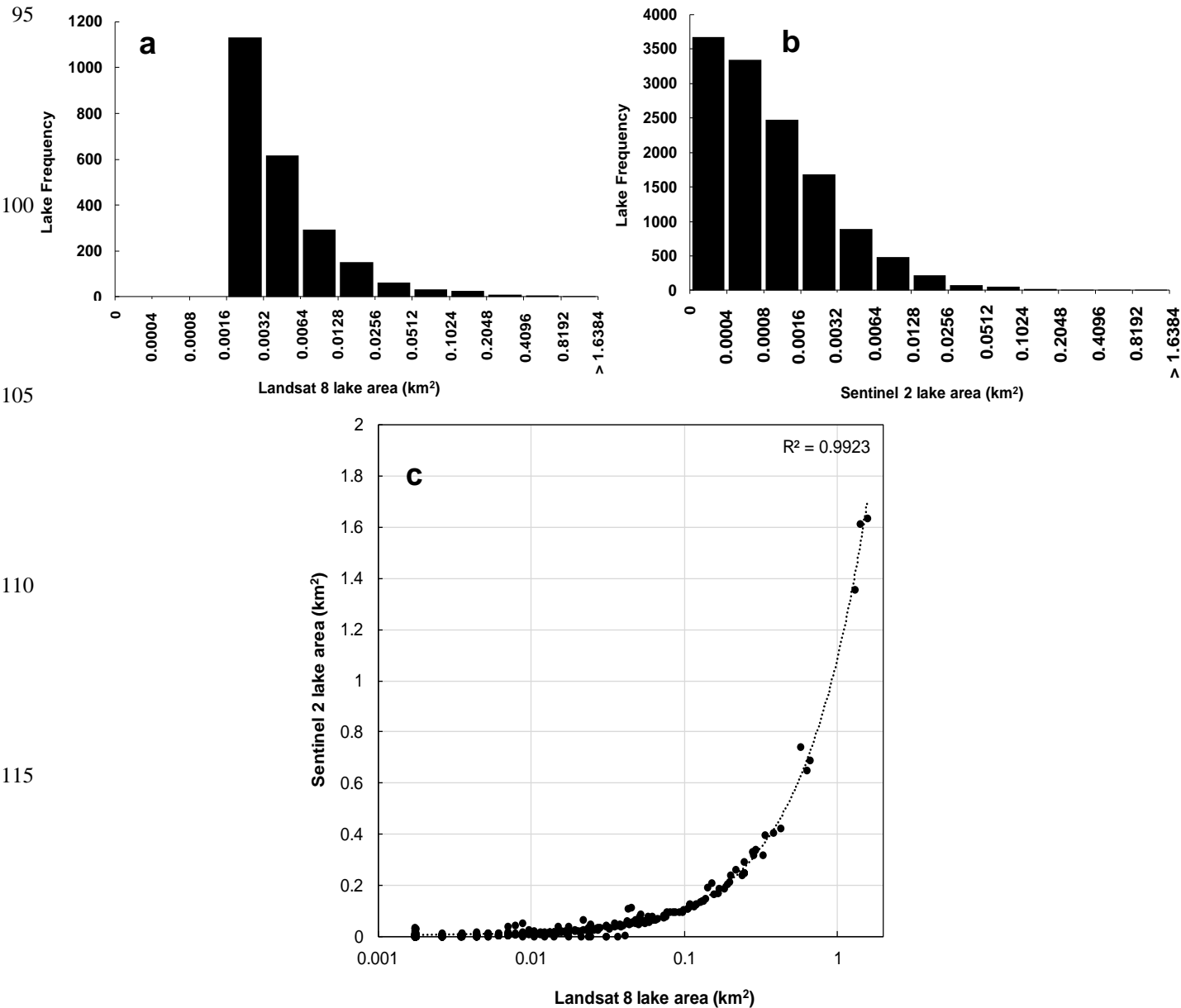
Supplementary Figure 1. Difference between different NDWI methods over an area snow-covered ice on which supraglacial lakes have formed (a - d) and exposed blue ice (e - h). The low near-infrared spectral reflectivity of snow-free blue ice results in pixels in blue ice areas being falsely classified as being water-covered. Background image is a Sentinel 2A image captured on 26th January 2018.



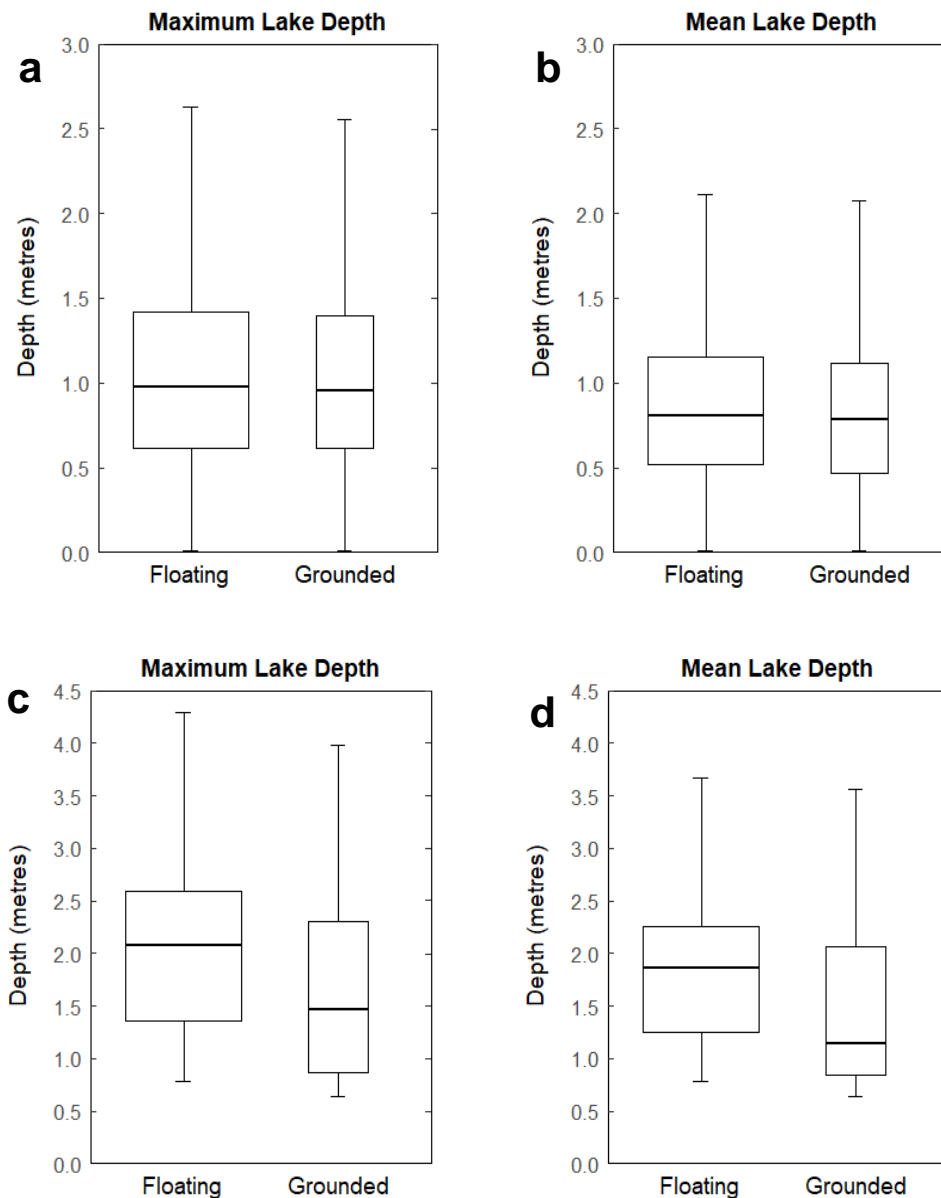
Supplementary Figure 2: Scatterplot of lake outlines comparing those derived from the Normalised Difference Water Index (black) to those derived from manual delineation (green) in four sample areas (a-d). Note the strong correlation of the linear regression ($R^2 = 0.979$), but with a higher scatter at very low lake areas. Lakes were manually delineated from a Landsat 8 scene (03/01/2014) in a-b and from a Sentinel 2 scene (19/01/2018) in c-d.

Assessing the effect of sensor resolution on lake detection and areas

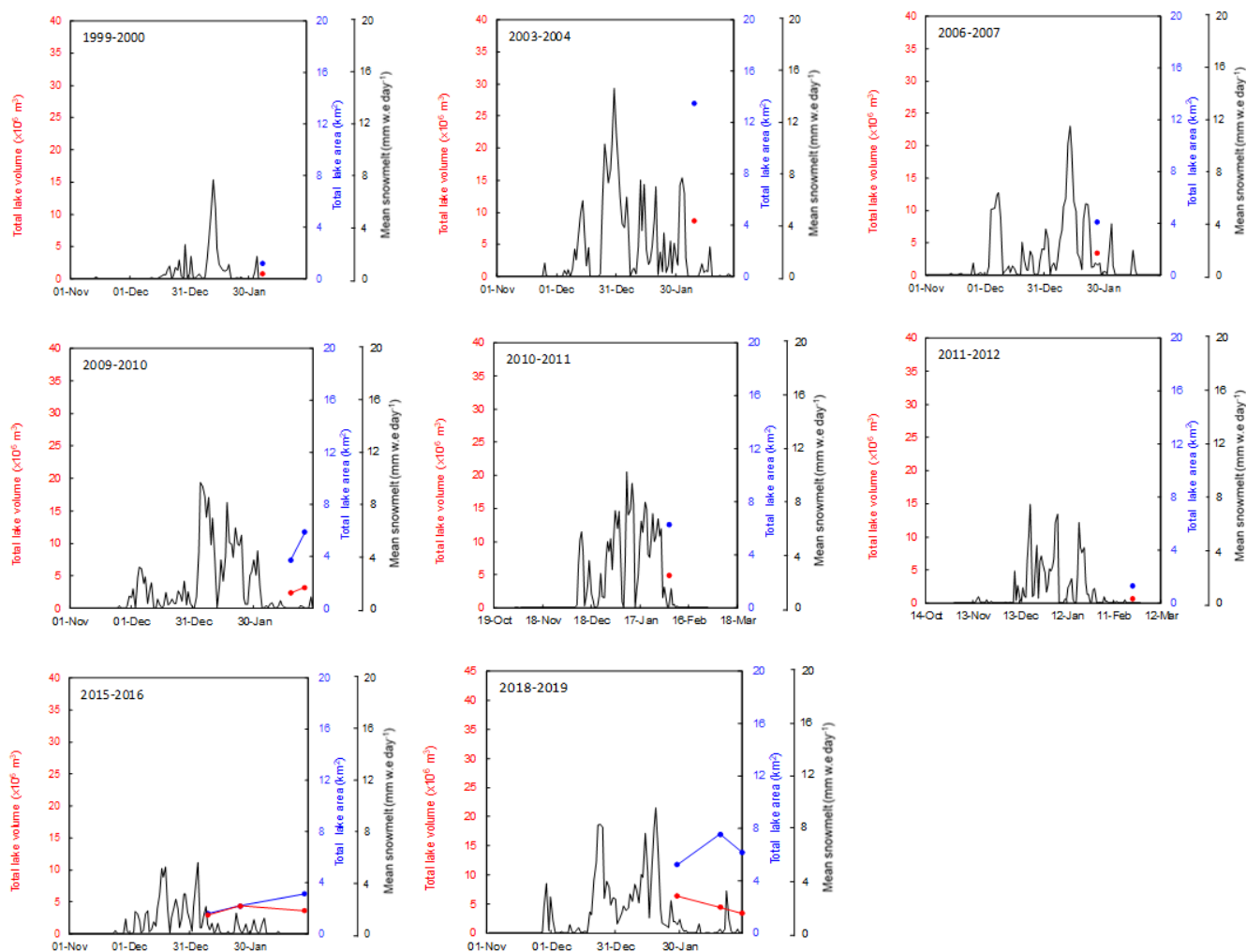
In order to assess the impact of sensor resolution on lake detection and lake extents, we extracted lake areas from the overlapping portion of a Sentinel 2B and Landsat 8 scene taken on 11th January 2020, using the NDWI (0.25 threshold) and a minimum size threshold of two pixels (see Section 3.2 of main paper). We detected larger numbers of smaller lakes from Sentinel 2B imagery (minimum of 200 m²) compared to Landsat 8 (minimum of 450 m²) (Supplementary Figure 3), but there is generally a very good agreement between lake areas derived from the two sensors ($R^2 = 0.9923$, $RMSE = 0.0003$). Lake areas derived from Sentinel 2 are generally higher, which we attribute to pixels along the outer edges of lakes being more accurately classified as water.



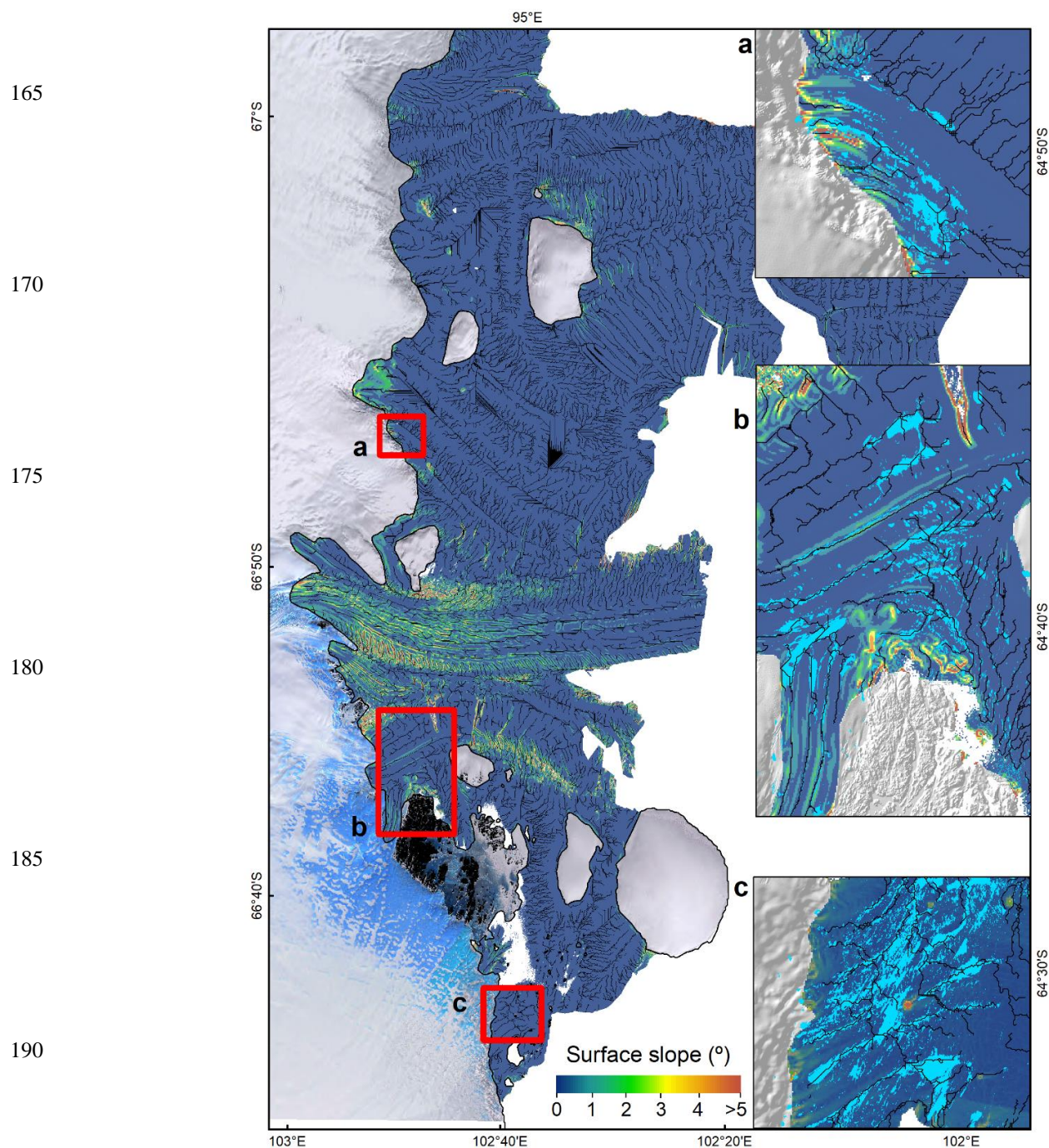
Supplementary Figure 3. Lake area-frequency distribution from a Landsat 8 scene on 11th January 2020 (a). Lake area-frequency distribution from the overlapping portion of a Sentinel 2 scene on 11th January 2020 (b). Scatterplot of Landsat 8 versus Sentinel 2 lake areas (c).



Supplementary Figure 4. Box plots of maximum depth and mean depth of SGLs on Shackleton Ice Shelf and on grounded ice within the sub-region (Figure 1, green box) from 2000 to 2020 (a, b) and from the date when the deepest lakes formed, 03/01/2014 (c, d). On each box, the bold line marks the median and the edges of the box are the 25th and 75th percentiles (q1 and q3). The length of the upper and lower whiskers is $q3 + 1.5 * (q3 - q1)$ and $q1 - 1.5 * (q3 - q1)$ respectively. Box widths are proportional to the number of lakes recorded on floating and grounded ice.



Supplementary Figure 5. Seasonal variations in total lake area, volume and modelled snowmelt for melt seasons with insufficient imagery to be able to determine whether peak area and volume follow a spike in surface melt. Snowmelt rates are mean values over the entire ice shelf.



Supplementary Figure 6. Predicted surface meltwater routing on Shackleton Ice Shelf (black channels) overlain by ice shelf surface slopes and by SGs mapped in this study (light blue), assuming widespread firn saturation across the ice shelf. Surface meltwater is predicted to be fed from higher slope areas upstream and converge in topographical lows, where it will be exported off the ice shelf along troughs. Insets show SGs mapped in this study closely correspond with predicted paths of meltwater routing.